Flat-Band-Enabled Triplet Excitonic Insulator in a Diatomic Kagome Lattice

Gurjyot Sethi, Yinong Zhou, Linghan Zhu, Li Yang, and Feng Liu

Phys. Rev. Lett. **126**, 196403 — Published 12 May 2021

DOI: 10.1103/PhysRevLett.126.196403

Flat-Bands-Enabled Triplet Excitonic Insulator in a Di-atomic Kagome Lattice

Gurjyot Sethi[1], Yinong Zhou[1], Linghan Zhu[2], Li Yang[2,3], and Feng Liu[1]
[1]*Department of Materials Science and Engineering, University of Utah, Salt Lake City, Utah 84112, USA*
[2]*Department of Physics, Washington University in St. Louis, St. Louis, Missouri, 63130, USA*
[3]*Institute of Materials Science and Engineering, Washington University in St. Louis, St. Louis, Missouri, 63130, USA*
(Dated: April 15, 2021)

The excitonic insulator (EI) state is a strongly correlated many-body ground state, arising from an instability in the band structure towards exciton formation. We show that the flat valence and conduction bands of a semiconducting diatomic Kagome lattice, as exemplified in a superatomic graphene lattice, can possibly conspire to enable an interesting triplet EI state, based on density functional theory (DFT) calculations combined with many-body GW and Bethe-Salpeter Equation (BSE). Our results indicate that massive carriers in flat bands with highly localized electron and hole wavefunctions significantly reduce the screening and enhance the exchange interaction, leading to an unusually large triplet exciton binding energy (∼1.1 eV) exceeding the GW band gap by ∼0.2 eV and a large singlet-triplet splitting of ∼0.4 eV. Our findings enrich once again the intriguing physics of flat bands and extend the scope of EI materials.

The discovery of excitonic insulator (EI) state has been a sought-after endeavor since it was first proposed by Kohn [1, 2] about fifty years ago. The EI phase is an exotic highly correlated electronic state that can be stabilized in narrow-gap semiconductors or semimetals [1–4] via spontaneous formation of excitons below a critical temperature (T_c). Originally Bardeen-Cooper-Schiefer (BCS) theory of superconductivity was used to model the EI state [1, 2] in the semi-metallic regime (negative band gap, E_g), where a high carrier density makes the electron-hole (e-h) Coulomb's attraction strongly screened for a suppressed T_c [5]. On the other hand, for semiconductors, if the exciton binding energy (E_b) exceeds E_g, a spontaneous Bose-Einstein condensation (BEC) of excitons triggers the formation of EI state, and the coherence in bosonic wavefunctions leads to super transport [4, 6] and a weaker screening increases T_c [7]. The study of EI state should give deeper insight into highly correlated phenomena like superconductivity and BEC-BCS crossover [8–10], and a plethora of theoretical and experimental investigations have been made in an effort to realize this state [7, 11–14]. However, difficulty arises when trying to experimentally identify it since the excitons are neutral species whose current is not straightforwardly measurable. This demands investigation into other experimental signatures of EI [7, 12–14].

The realization of an EI requires highly reduced screening to Coulomb's potential that leads to a higher E_b. Low-dimensional materials tend to have reduced screening [15, 16] due to confinement effect. While two-dimensional (2D) semiconductors with a small E_g may have lower E_b because polarizability is inversely related to E_g [17], dipole forbidden transitions near the band edges are shown to break this synergy and favor the formation of an intrinsic EI state, such as in 2D GaAs [18] and Graphone [19]. Another natural way of reducing screening is by increasing the e-h wavefunction overlap [20–22], which brings electrons and holes closer making them immune to the screening effect from surrounding charges.

Triplet EI state is especially appealing, because triplet excitons carry spin current so that a triplet EI with spin superfluidity can be experimentally observed by spin transport measurements [23]. Triplet excitons are also attracting increasing attention in photovoltaics owing to their high radiative lifetime [24, 25]. Due to optical selection rule [26], the triplet excitons are dark but may be converted from singlets by intersystem crossing [27, 28]. A large singlet-triplet splitting (ΔE_{ST}) will favor such crossing process and increase the triplet concentration at finite temperatures [29–33]. Hence, a large e-h wavefunction overlap is especially desirable for the triplet EI formation because it increases ΔE_{ST} [30, 31] by enhancing the e-h exchange interaction [34].

In this Letter, we demonstrate an intriguing FBs-enabled mechanism that can possibly lead to the formation of triplet EI mediated by massive carriers with greatly enhanced e-h wavefunction localization and overlap in a 2D diatomic (Yin-Yang) Kagome lattice [35], and further predict its realization in a real material made of superatomic graphene. Intrinsic to a topological flat band (FB) is its highly localized wavefunction in real space, underlined by a destructive interference of FB quantum states [36]. When a unique band-structure configuration arises, with both a topological valence and conduction FB separated by a trivial gap, it also indicates an extremely high degree of e-h wavefunction overlap. Remarkably, the huge effective masses of carriers hosted in the two FBs greatly reduce the screening to increase exciton E_b, favoring the formation of EI states in general; while the highly overlapping e-h wavefunction enhances the Coulomb's direct interaction on the one hand, to further reduce the screening, and the exchange interaction on the other hand, to increase ΔE_{ST}, favoring the formation of triplet EI states in specific. Using a superatomic graphene lattice as a prototypical example, we show the possibility of a FBs-enabled triplet EI state, based on DFT calculations combined with many-body GW and

BSE. This is indicated by a triplet exciton E_b (∼1.1 eV) exceeding the GW gap (E_g ∼0.9 eV) by ∼20% and a high ΔE_{ST} (∼0.4 eV). FBs also provide an ideal platform for BEC and coherence [37] since the macroscopic degeneracy of FBs can lead to spontaneous symmetry breaking which is central to the theory of BCS superconductivity [38, 39] and EI [40, 41].

Fig. 1(a) shows the structure of the superatomic graphene lattice. It consists of two 9×9 grpahene flakes (structural motif) with an optimized lattice constant of 22.14 Å. This peculiar structural motif enables the C atomic p_z orbitals to hybridize into molecular sp^2 orbitals, forming the so-called Yin-Yang Kagome bands [35] in a hexagonal lattice, as shown in Fig. 1(c). Both the highest valence and the lowest conduction bands are perfectly flat and topologically nontrivial with opposite spin Chern numbers [35]. The structure has a high thermodynamic stability with a bulk cohesive energy calculated as -6.78 eV per atom [42], similar to graphene nanoribbon [43]. Excitingly, recent experimental advances [44, 45] in synthesizing nano-porous graphene suggest very high feasibility of making this lattice. These latest experiments employ a bottom-up approach to successfully make artificial nano-porous graphene lattices with precise control of pore size and shape, using designed molecular precursors. Accordingly, our theoretical study should stimulate such experimental efforts to make the proposed lattice by designing the desired superatomic graphene precursors. Also, other Ying-Yang Kagome lattices, such as the Kagome super-lattices formed in Moire pattern twisted graphene bilayers [46], which generated a lot of recent interest, can be generally explored. Here we focus on the exciton related properties of the 9×9 superatomic graphene lattice.

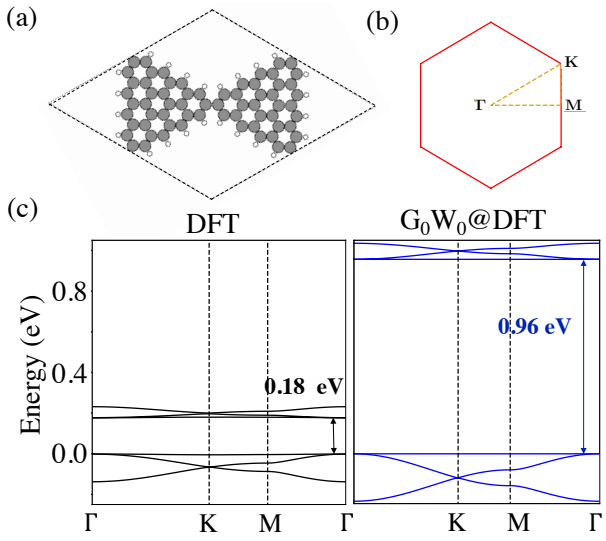

FIG. 1. (a) Unit cell of a 9 × 9 superatomic graphene lattice. Grey and white circles represent C and H atoms, respectively. (b) First Brillouin zone showing the high-symmetry reciprocal paths used for band diagrams. (c) Comparison of band structures and band gaps obtained within DFT (left panel) and a single-shot G_oW_o calculation (right).

First, its mean-field DFT E_g∼0.18 eV, as in a narrow-gap semiconductor, is significantly corrected to a GW E_g∼0.94 eV (Fig. 1(c)). The optical spectra obtained by solving BSE is shown in Fig. 2(a), in comparison with that obtained within the independent particle approximation. The first peak in the BSE spectra corresponds to the first bright singlet exciton at 0.24 eV, marked by X_o. This can also be seen from the density of states (DOS) for singlet excitons in Fig. 2(b). The formation energy of X_o is very low compared to the quasiparticle gap of 0.94 eV, giving rise to a large E_b of 0.70 eV. In Fig. 2(c), we plot the DOS for triplet excitons which clearly shows the presence of excitons with negative formation energy, indicative of spontaneous formation of excitons. The E_b of the lowest triplet exciton (0.94 eV + 0.17 eV = 1.11 eV) exceeds the GW gap by 0.17 eV, to signify a desired property for a strong triplet EI state, as marked by EI_o in Fig. 2(c). This possible triplet EI in a non-magnetic material is different from that recently studied in a ferromagnetic material where the excitation between spin non-degenerate bands was considered [19]. One interesting feature is its huge ΔE_{ST} of 0.41 eV, making it easier to be detected by spin superfluidity experiment [23]. In Table I we summarize the energies of the lowest singlet (X_o) and triplet (EI_o) states. The key result of a negative triplet exciton formation energy is carefully confirmed by convergence tests for GW-BSE calculations (see Table S1-S5 [42]).

Excitonic instability may occur in either a narrow-gap semiconductor or a semimetal [47]. In the former, a gapped system as studied here, the critical condition for the existence of EI state is a negative exciton forma-

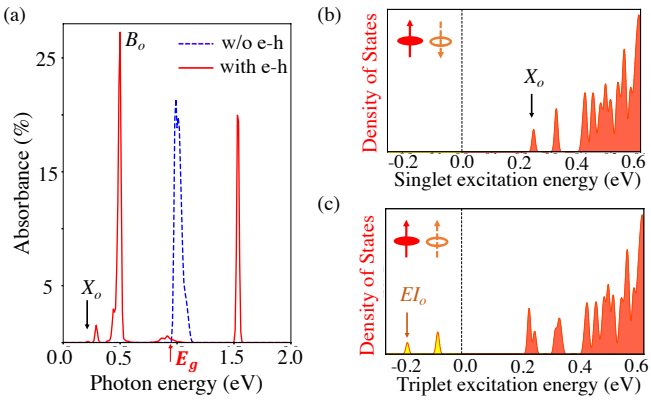

FIG. 2. (a) Optical absorbance for singlet excitons with a Gaussian peak broadening of 10 meV. X_o indicates the first bright peak. (b) Density of states for singlet excitons, and (c) Density of states for triplet excitons, noticing two peaks with negative formation energies (yellow-filled). EI_o indicates the first triplet exciton which is also the case of triplet EI. Insets in (b) and (c) represent spin-up electron (red arrow with filled circle) and spin-down hole (orange arrow with hollow circle) bound together forming an exciton.

TABLE I. Summary of excitonic energies for states X_o and EI_o. Last column denotes the dipole oscillator strength of excitons divided by the number of k-points.

Exciton	Mean field gap (eV)	GW band gap (eV)	Excitation energy (eV)	Binding energy (eV)	Dipole Oscillator strength/N_k (μ_s)
Singlet (X_o)	0.18	0.96	0.21	0.75	0.024 au
Triplet (EI_o)	0.18	0.96	-0.21	1.17	-

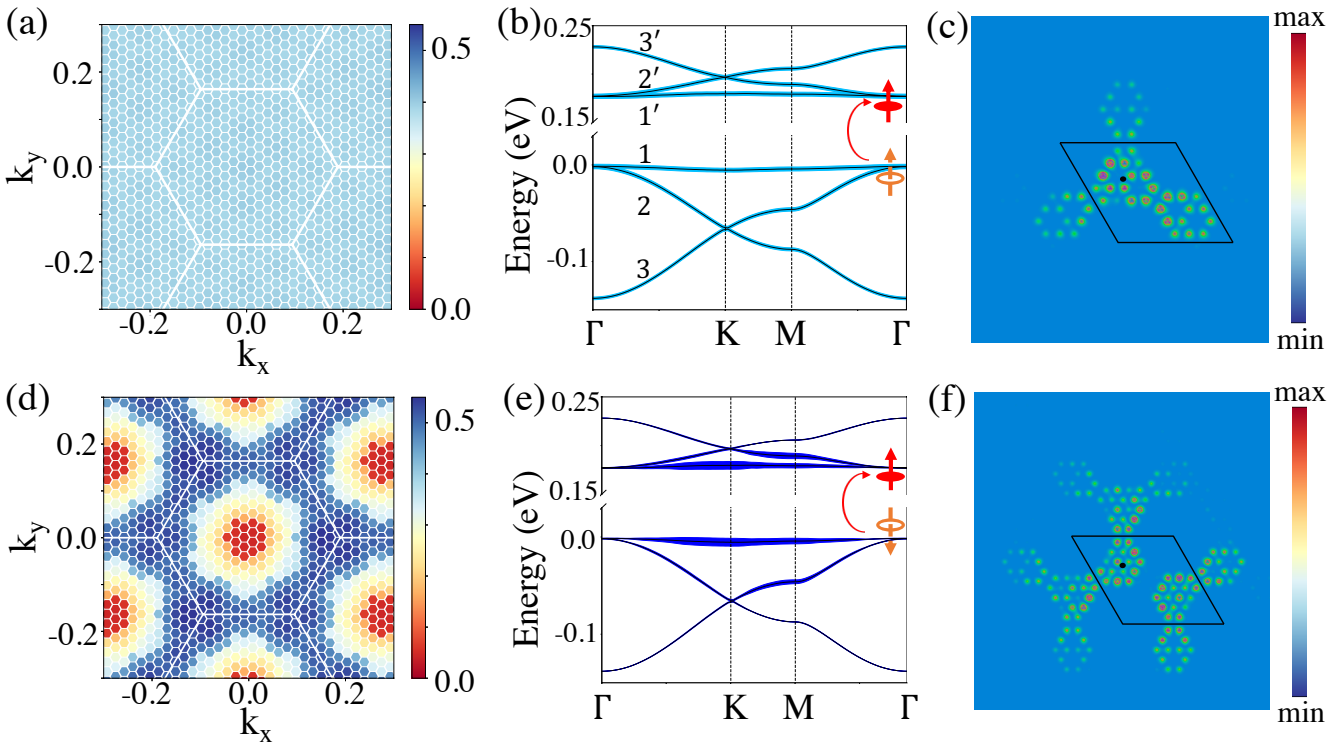

FIG. 3. Excitonic wavefunction analysis for the lowest triplet exciton (EI_o, Upper panel) and for the lowest singlet exciton (X_o, lower panel): (a), (d) Reciprocal-space excitonic wavefunction distribution showing total contribution of all excitations at each reciprocal lattice point, (b), (e) Band excitation contributions indicated by spread of color on the bands, (c), (f) Real space two-particle e-h wavefunction distribution with hole fixed at the black dot plotted over a 6×6 supercell. Only a small segment of the supercell is shown here since the electron is highly localized around the hole. The distribution amplitude is zero everywhere else. The orange arrow with a circle denotes the spin of hole left behind after excitation and the red arrow denotes the spin of electron.

tion energy, i.e., if E_b exceeds E_g, the order parameter for BEC of excitons has a non-trivial solution at low temperatures. In a two-band model, the order parameter at T= 0 K is given by $\Delta_0 = E_b\sqrt{(\frac{1}{2} - \frac{E_g}{2E_b})}$ [47]. As long as E_b>E_g, Δ_0 is finite positive and a BEC-EI state emerges below T_c. Our calculated E_b is ∼20% larger than E_g, indicating a relatively high T_c. For a system with parabolic valence and conduction bands, T_c may be estimated from a $k.p$ effective-mass model [19]. However, this model is not applicable to FBs with infinite effective mass, instead an extensive exact diagonalization approach is required to determine T_c. Differently in a semimetal, the EI state occurs below T_c' via a metal (gapless) to insulator (gapped) transition, a manifestation of spontaneous symmetry breaking [2, 47]. It further involves a BCS-BEC crossover depending on the e-h coupling strength [48]. One widely studied material for semimetal-to-EI transition is Ta_2NiSe_5, and a recent work [41] shows that such transition may be generally triggered by a structural transition with breaking of lattice symmetries. Also, the BEC-BCS crossover has been studied in the context of non-equilibrium EI state [49].

In order to better understand the strikingly enhanced E_b, suggestive of the formation of triplet EI ground state below T_c, we plot the excitonic wavefunction in reciprocal space and band excitation contributions for EI_o in Fig. 3(a) and Fig. 3(b), respectively. One clearly sees that EI_o is composed of coherent excitations throughout the Brillouin zone (BZ). We also examined relative band contributions to the excitations (see Table S6 [42]). The contribution from valence to conduction FB excitation

is slightly higher than from other excitations. The nature of FB excitations inherently implies localized wavefunctions in real space as seen in Fig. 3(c), which shows the Fourier transform of excitonic wavefunction for EI_o, consistent with the broad distribution of k-point-resolved excitations (Fig. S1 [42]). This provides additional evidence for a possible BEC-EI state, because the triplet exciton width (ξ) is much smaller than the lattice constant, implying a point-like boson, as in the BEC condensate [49–51]. In comparison, for X_o, as shown in Fig. 3(d)-(e), excitation from valence to conduction FB contributes the most, largely centered around the K point. The triplet EI_o state has an even more localized wavefunction in real space (Fig. 3(c)) than the singlet X_o (Fig. 3(f)), because the former is excited throughout the BZ, i.e., the excitonic wavefunction is highly delocalized in reciprocal space.

The effective static dielectric constant obtained from our calculations is unusually low ∼1.02, indicating a highly reduced screening, which is a direct manifestation of FB wavefunctions as we show below. Usually dipole forbidden transitions near the band edges are favored for large E_b, and hence the formation of EI state [17–19]. For the Yin-Yang FBs, the inter-FB transitions are actually allowed by symmetry [35] but the band flatness makes the dipole matrix element between them negligible. Considering a two-band model, the dipole matrix element is given by,

$$| < u_{c,k}|\nabla_k|u_{v,k} > |^2 = \frac{\hbar^2}{2\mu}(E_g + \frac{\hbar^2 k^2}{2\mu})^{-1} \qquad (1)$$

where μ is the reduced mass under the effective mass approximation [17], which is very high here for both valence and conduction FBs making the above expression close to zero. A negligible dipole matrix element is directly verified from the absence of absorption peak at E_g in the optical spectrum (Fig. 2(a)) obtained within the independent particle approximation (see also Fig. S4 [42]). This also explains the very low absorbance for X_o (Fig. 2(a)) since the major contribution to this state is from FB excitations, and its non-zero portion of absorption is mostly contributed by weaker transitions that involve parabolic bands (e.g., 1→2′ near M point) as shown in Fig. 3(e). Basically, only parabolic-band transitions lead to high optical absorption. The detailed contributions from individual band excitations are available in supplementary material [42] (Table S1 and Fig. S2), and the band resolved contributions to the brightest exciton, marked in Fig. 2(a) by B_o, is available in Fig. S3 [42]. Since 2D polarizability is proportional to the dipole matrix element divided by the gap [17], the presence of FBs as both the highest occupied valence and the lowest unoccupied conduction bands inherently reduces the screening significantly.

Normally, reduced screening and confinement effects in low dimensions are known to extrinsically increase the e-h wavefunction overlap as shown in hetero-nanostructures [29] and carbon nanotubes [30]. Interestingly here both electron and hole wavefunctions exhibit a form of destructive quantum interference originated from the FB topology [36], which gives rise to their distinguished localized states in real space with huge overlap. Fig. 4 shows the relative overlap between the two FB wavefunctions at high-symmetry k-points projected over atomic orbitals of C and H. Such huge overlap leads to a much higher energy for singlet compared to triplet excitons as the exchange interaction is absent in the latter. This represents a unique *intrinsic* FB originated increase of direct and exchange energy, leading to a ΔE_{ST} of ∼0.4 eV, much larger than the typical values in bulk (a few meVs) [29] and low-dimensional semiconductors (upto ∼0.2 eV) [30–33]. Thus, both a huge e-h wavefunction overlap and a highly reduced screening, as induced by the FBs, are the major factors leading to a large E_b, and an enhanced ΔE_{ST}, favorable for a triplet EI. More singlet exciton properties are given in SM [42].

For comparison, it might be interesting to construct a supermolecule consisting of two superatomic graphene flakes and study its excitonic properties, for which a Frenkel type of localized exciton is expected. Also, in the condensed state of Van der Waals molecular crystals, excitons with relatively large E_b and almost linear excitonic dispersion have been previously shown [52]. In contrast, for the covalently bonded framework we study here, the highly localized and overlapping exciton wavefunctions, as shown in Fig. 3(c) and Fig. 3(f), are enabled by FBs, having a very different physical origin. This is because the FB is a Bloch state; it is encoded with non-

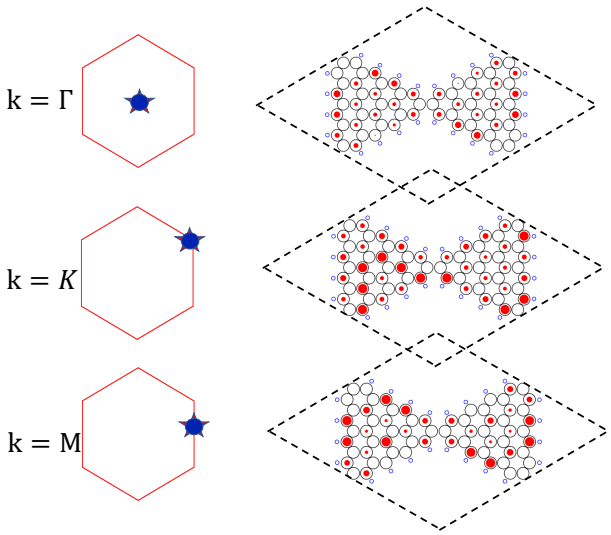

FIG. 4. Conduction and valence FBs wavefunction overlap for zero momentum singlet exciton (Q = 0). Right: C and H atoms are indicated by large and small circles respectively. The contributions are only from the C p_z orbitals. The overlapped weights of these contributions to flat valence and conduction bands wavefunctions are indicated by the size of red fills on the C atoms. Left: k-points in BZ for which overlaps are calculated.

trivial topology, arising from destructive interference of lattice hopping that leads to compact plaquette states of both electrons and holes in real space [35]. As such, the excitons display an unusual constant dispersion (see also the discussion for singlet excitons in SM [42]).

In conclusion, we reveal a unique topological FB-originated mechanism for the possible formation of a spin triplet EI, making a significant forward step for the discovery of EIs through spin transport measurement. In a 9×9 superatomic graphene lattice, a triplet exciton E_b is predicted to exceed the band gap by $\sim$0.2 eV. The FBs, generally existing in a Yin-Yang Kagome lattice, weaken intrinsically the screened e-h interaction by an infinite effective mass of carriers and a complete overlap of e-h wavefunctions, and the latter also increases the exchange energy of singlet exciton leading to a huge ΔE_{ST}. In general, defects are likely present in experimental samples. However, if the defect density is kept low, there is usually no significant change in the screening and excitonic properties, as shown in transition metal dichalcogenides [53]. Spin-orbit coupling (SOC) may have interesting consequences in our proposal; however, since only C and H atoms are present here, it is negligible and not considered. Other Ying-Yang Kagome lattice materials with large SOC are interesting topics of future studies, especially in considering the related phenomena of excited quantum anomalous and spin Hall effect [35]. Furthermore, fractional population of two FBs may lead to exotic fractional EI state [54].

G.S, Y.Z. and F.L. acknowledge financial support from US Department of Energy-Basic Energy Sciences (Grant No. DE-FG02- 04ER46148). L.Z. and L.Y. are supported by the Air Force Office of Scientific Research (AFOSR) grant No. FA9550-20-1-0255 and the National Science Foundation (NSF) CAREER grant No. DMR-1455346. The calculations were done on the CHPC at the University of Utah and DOE-NERSC.

[1] W. Kohn, Excitonic phases, Physical Review Letters **19**, 439 (1967).
[2] D. Jérome, T. Rice, and W. Kohn, Excitonic insulator, Physical Review **158**, 462 (1967).
[3] N. F. Mott, The transition to the metallic state, Philosophical Magazine **6**, 287 (1961).
[4] B. Halperin and T. Rice, Possible anomalies at a semimetal-semiconductor transition, Reviews of Modern Physics **40**, 755 (1968).
[5] F. X. Bronold and H. Fehske, Possibility of an excitonic insulator at the semiconductor-semimetal transition, Physical Review B **74**, 165107 (2006).
[6] W. Kohn and D. Sherrington, Two kinds of bosons and bose condensates, Reviews of Modern Physics **42**, 1 (1970).
[7] Y. Lu, H. Kono, T. Larkin, A. Rost, T. Takayama, A. Boris, B. Keimer, and H. Takagi, Zero-gap semiconductor to excitonic insulator transition in ta_2nise_5, Nature communications **8**, 1 (2017).
[8] V.-N. Phan, K. W. Becker, and H. Fehske, Spectral signatures of the bcs-bec crossover in the excitonic insulator phase of the extended falicov-kimball model, Physical Review B **81**, 205117 (2010).
[9] B. Zenker, D. Ihle, F. Bronold, and H. Fehske, Electron-hole pair condensation at the semimetal-semiconductor transition: A bcs-bec crossover scenario, Physical Review B **85**, 121102 (2012).
[10] K. Seki, Y. Wakisaka, T. Kaneko, T. Toriyama, T. Konishi, T. Sudayama, N. Saini, M. Arita, H. Namatame, M. Taniguchi, *et al.*, Excitonic bose-einstein condensation in ta_2nise_5 above room temperature, Physical Review B **90**, 155116 (2014).
[11] B. Bucher, P. Steiner, and P. Wachter, Excitonic insulator phase in $tmse_{0.45}te_{0.55}$, Physical review letters **67**, 2717 (1991).
[12] Y. Wakisaka, T. Sudayama, K. Takubo, T. Mizokawa, M. Arita, H. Namatame, M. Taniguchi, N. Katayama, M. Nohara, and H. Takagi, Excitonic insulator state in ta_2nise_5 probed by photoemission spectroscopy, Physical review letters **103**, 026402 (2009).
[13] L. Du, X. Li, W. Lou, G. Sullivan, K. Chang, J. Kono, and R.-R. Du, Evidence for a topological excitonic insulator in inas/gasb bilayers, Nature communications **8**, 1 (2017).
[14] Z. Li, M. Nadeem, Z. Yue, D. Cortie, M. Fuhrer, and X. Wang, Possible excitonic insulating phase in quantum-confined sb nanoflakes, Nano letters **19**, 4960 (2019).
[15] A. Chernikov, T. C. Berkelbach, H. M. Hill, A. Rigosi, Y. Li, O. B. Aslan, D. R. Reichman, M. S. Hybertsen, and T. F. Heinz, Exciton binding energy and nonhydrogenic rydberg series in monolayer ws_2, Physical review letters **113**, 076802 (2014).
[16] P. Cudazzo, L. Sponza, C. Giorgetti, L. Reining, F. Sottile, and M. Gatti, Exciton band structure in two-dimensional materials, Physical review letters **116**, 066803 (2016).
[17] Z. Jiang, Z. Liu, Y. Li, and W. Duan, Scaling universality between band gap and exciton binding energy of two-dimensional semiconductors, Physical review letters **118**, 266401 (2017).
[18] Z. Jiang, Y. Li, S. Zhang, and W. Duan, Realizing an intrinsic excitonic insulator by decoupling exciton binding energy from the minimum band gap, Physical Review B **98**, 081408 (2018).
[19] Z. Jiang, W. Lou, Y. Liu, Y. Li, H. Song, K. Chang, W. Duan, and S. Zhang, Spin-triplet excitonic insulator: The case of semihydrogenated graphene, Physical Review Letters **124**, 166401 (2020).
[20] J.-C. Blancon, A. V. Stier, H. Tsai, W. Nie, C. C. Stoumpos, B. Traore, L. Pedesseau, M. Kepenekian, F. Katsutani, G. Noe, *et al.*, Scaling law for excitons in 2d perovskite quantum wells, Nature communications **9**, 1 (2018).
[21] W. Wei, Y. Dai, B. Huang, and T. Jacob, Enhanced many-body effects in 2- and 1-dimensional zno structures: A green's function perturbation theory study, The Journal of Chemical Physics **139**, 144703 (2013).
[22] M. Goryca, J. Li, A. V. Stier, T. Taniguchi, K. Watanabe,

E. Courtade, S. Shree, C. Robert, B. Urbaszek, X. Marie, *et al.*, Revealing exciton masses and dielectric properties of monolayer semiconductors with high magnetic fields, Nature communications **10**, 1 (2019).
[23] Q.-f. Sun, Z.-t. Jiang, Y. Yu, and X. Xie, Spin superconductor in ferromagnetic graphene, Physical Review B **84**, 214501 (2011).
[24] B. T. Luppi, D. Majak, M. Gupta, E. Rivard, and K. Shankar, Triplet excitons: improving exciton diffusion length for enhanced organic photovoltaics, Journal of Materials Chemistry A **7**, 2445 (2019).
[25] M. Einzinger, T. Wu, J. F. Kompalla, H. L. Smith, C. F. Perkinson, L. Nienhaus, S. Wieghold, D. N. Congreve, A. Kahn, M. G. Bawendi, *et al.*, Sensitization of silicon by singlet exciton fission in tetracene, Nature **571**, 90 (2019).
[26] T. Mueller and E. Malic, Exciton physics and device application of two-dimensional transition metal dichalcogenide semiconductors, npj 2D Materials and Applications **2**, 1 (2018).
[27] J. Palotás, M. Negyedi, S. Kollarics, A. Bojtor, P. Rohringer, T. Pichler, and F. Simon, Incidence of quantum confinement on dark triplet excitons in carbon nanotubes, ACS nano **14**, 11254 (2020).
[28] M. Kasha, Characterization of electronic transitions in complex molecules, Discussions of the Faraday society **9**, 14 (1950).
[29] H. Fu, L.-W. Wang, and A. Zunger, Excitonic exchange splitting in bulk semiconductors, Physical Review B **59**, 5568 (1999).
[30] A. Granados Del Águila, E. Groeneveld, J. C. Maan, C. de Mello Donegá, and P. C. Christianen, Effect of electron–hole overlap and exchange interaction on exciton radiative lifetimes of cdte/cdse heteronanocrystals, ACS nano **10**, 4102 (2016).
[31] V. Perebeinos, J. Tersoff, and P. Avouris, Radiative lifetime of excitons in carbon nanotubes, Nano Letters **5**, 2495 (2005).
[32] M. Nirmal, D. J. Norris, M. Kuno, M. G. Bawendi, A. L. Efros, and M. Rosen, Observation of the" dark exciton" in cdse quantum dots, Physical review letters **75**, 3728 (1995).
[33] D. J. Norris, A. L. Efros, M. Rosen, and M. G. Bawendi, Size dependence of exciton fine structure in cdse quantum dots, Physical Review B **53**, 16347 (1996).
[34] M. Rohlfing and S. G. Louie, Electron-hole excitations and optical spectra from first principles, Physical Review B **62**, 4927 (2000).
[35] Y. Zhou, G. Sethi, H. Liu, Z. Wang, and F. Liu, Excited quantum hall effect: enantiomorphic flat bands in a yin-yang kagome lattice, arXiv preprint arXiv:1908.03689 (2019).
[36] L. Zheng, L. Feng, and W. Yong-Shi, Exotic electronic states in the world of flat bands: From theory to material, Chinese Physics B **23**, 077308 (2014).
[37] S. D. Huber and E. Altman, Bose condensation in flat bands, Physical Review B **82**, 184502 (2010).
[38] S. Weinberg, *The quantum theory of fields*, Vol. 2 (Cambridge university press, 1995).
[39] S. Weinberg, Superconductivity for particular theorists, PThPS **86**, 43 (1986).
[40] T. Kaneko, K. Seki, and Y. Ohta, Excitonic insulator state in the two-orbital hubbard model: Variational cluster approach, Physical Review B **85**, 165135 (2012).
[41] G. Mazza, M. Rösner, L. Windgätter, S. Latini, H. Hübener, A. J. Millis, A. Rubio, and A. Georges, Nature of symmetry breaking at the excitonic insulator transition: Ta_2nise_5, Physical Review Letters **124**, 197601 (2020).
[42] See supplementary material at for details, which includes refs. [55–63].
[43] V. Barone, O. Hod, and G. E. Scuseria, Electronic structure and stability of semiconducting graphene nanoribbons, Nano letters **6**, 2748 (2006).
[44] P. H. Jacobse, R. D. McCurdy, J. Jiang, D. J. Rizzo, G. Veber, P. Butler, R. Zuzak, S. G. Louie, F. R. Fischer, and M. F. Crommie, Bottom-up assembly of nanoporous graphene with emergent electronic states, Journal of the American Chemical Society **142**, 13507 (2020).
[45] C. Moreno, M. Vilas-Varela, B. Kretz, A. Garcia-Lekue, M. V. Costache, M. Paradinas, M. Panighel, G. Ceballos, S. O. Valenzuela, D. Peña, *et al.*, Bottom-up synthesis of multifunctional nanoporous graphene, Science **360**, 199 (2018).
[46] A. Ramires and J. L. Lado, Electrically tunable gauge fields in tiny-angle twisted bilayer graphene, Physical review letters **121**, 146801 (2018).
[47] A. Kozlov and L. Maksimov, The metal-dielectric divalent crystal phase transition, Sov. Phys. JETP **2**, 790 (1965).
[48] K. Sugimoto, S. Nishimoto, T. Kaneko, and Y. Ohta, Strong coupling nature of the excitonic insulator state in ta_2nise_5, Physical review letters **120**, 247602 (2018).
[49] E. Perfetto, D. Sangalli, A. Marini, and G. Stefanucci, Time-resolved arpes signatures of pump driven normal-to-excitonic insulator transition, Bulletin of the American Physical Society **65** (2020).
[50] T. Kaneko, S. Ejima, H. Fehske, and Y. Ohta, Exact-diagonalization study of exciton condensation in electron bilayers, Physical Review B **88**, 035312 (2013).
[51] T. Kaneko, Theoretical study of excitonic phases in strongly correlated electron systems, Chiba University (2016).
[52] P. Cudazzo, F. Sottile, A. Rubio, and M. Gatti, Exciton dispersion in molecular solids, Journal of Physics: Condensed Matter **27**, 113204 (2015).
[53] S. Refaely-Abramson, D. Y. Qiu, S. G. Louie, and J. B. Neaton, Defect-induced modification of low-lying excitons and valley selectivity in monolayer transition metal dichalcogenides, Physical review letters **121**, 167402 (2018).
[54] Y. Hu, J. W. Venderbos, and C. Kane, Fractional excitonic insulator, Physical review letters **121**, 126601 (2018).
[55] J. P. Perdew, K. Burke, and M. Ernzerhof, Generalized gradient approximation made simple, Physical review letters **77**, 3865 (1996).
[56] P. Giannozzi, S. Baroni, N. Bonini, M. Calandra, R. Car, C. Cavazzoni, D. Ceresoli, G. L. Chiarotti, M. Cococcioni, I. Dabo, *et al.*, Quantum espresso a modular and open-source software project for quantum simulations of materials, Journal of physics: Condensed matter **21**, 395502 (2009).
[57] J. Deslippe, G. Samsonidze, D. A. Strubbe, M. Jain, M. L. Cohen, and S. G. Louie, Berkeleygw a massively parallel computer package for the calculation of the quasiparticle and optical properties of materials and nanos-

tructures, Computer Physics Communications **183**, 1269 (2012).
[58] M. S. Hybertsen and S. G. Louie, Electron correlation in semiconductors and insulators: Band gaps and quasiparticle energies, Physical Review B **34**, 5390 (1986).
[59] M. Rohlfing and S. G. Louie, Electron-hole excitations and optical spectra from first principles, Physical Review B **62**, 4927 (2000).
[60] V. Barone, O. Hod, and G. E. Scuseria, Electronic structure and stability of semiconducting graphene nanoribbons, Nano letters **6**, 2748 (2006).
[61] R. Gillen and J. Maultzsch, Light-matter interactions in two-dimensional transition metal dichalcogenides: Dominant excitonic transitions in mono-and few-layer mox_2 and band nesting, IEEE Journal of Selected Topics in Quantum Electronics **23**, 219 (2016).
[62] M. Palummo, M. Bernardi, and J. C. Grossman, Exciton radiative lifetimes in two-dimensional transition metal dichalcogenides, Nano letters **15**, 2794 (2015).
[63] C. D. Spataru, S. Ismail-Beigi, R. B. Capaz, and S. G. Louie, Theory and ab initio calculation of radiative lifetime of excitons in semiconducting carbon nanotubes, Physical review letters **95**, 247402 (2005).